

Evidence for Vortices in the Pseudogap Region of $Y_{1-x}Pr_xBa_2Cu_3O_7$ from Angular Magnetoresistivity Measurements

V. Sandu,^{1,*} E. Cimpoiasu,^{1,†} T. Katuwal,¹ Shi Li,² M. B. Maple,² and C. C. Almasan¹

¹*Department of Physics, Kent State University, Kent, OH 44242, USA*

²*Department of Physics, University of California at San Diego, La Jolla, CA, USA*

(Received 12 August 2003; published 20 October 2004)

In-plane angular magnetoresistivity $\Delta\rho_{ab}^{\text{anis}}$ measurements were made on $Y_{1-x}Pr_xBa_2Cu_3O_{7-\delta}$ single crystals in the pseudogap region. For $x \geq 0.2$ single crystals, $\Delta\rho_{ab}^{\text{anis}}(\theta)$ displays a deviation from the typical quasiparticle contribution ($\propto \sin^2\theta$) for temperatures smaller than a certain value T_ϕ in the pseudogap region. This deviation is consistent with a flux-flow type contribution to angular magnetoresistivity, indicating the presence of vortexlike excitations above the zero-field critical temperature in the pseudogap region.

DOI: 10.1103/PhysRevLett.93.177005

PACS numbers: 74.25.Fy, 71.30.+h, 74.72.Bk, 75.47.Gk

Starting with the seminal work of Abrikosov [1], vortex matter has been a continuous source of new research that suddenly exploded after the discovery of the high transition temperature oxide superconductors. More recently, the presence of vortices above the zero-field critical temperature T_{c0} was predicted in an attempt to depict the pseudogapped state as a system of quasiparticles interacting with thermally excited unbound vortices and antivortices [2–5]. Several investigations of superconducting cuprates have revealed responses above T_{c0} , which appear to indicate the presence of vortices; i.e., high frequency conductivity [6] on an underdoped $Bi_2Sr_2CaCu_2O_7$ single crystal has revealed the existence of short phase correlation times above T_{c0} , Nernst effect measurements [7] have revealed the presence of a Nernst signal in underdoped $La_{1-x}Sr_xCuO_4$ and $YBa_2Cu_3O_y$ above T_{c0} , while magnetization [8] has shown an anomalous fluctuation diamagnetism and irreversibility in $Y_{1-x}Ca_xBa_2Cu_3O_y$ for $T > T_{c0}$. A question that still remains is whether these signatures are a result of the presence of vortices above the zero-field critical temperature or of other effects. Evidence for the presence of vortices above T_{c0} has not yet been acquired in magnetotransport measurements, a technique that, in principle, is a direct way to detect vortex dissipation. Such measurements are imperative in resolving this issue.

In this Letter, we show evidence for vortices at temperatures well above T_{c0} , in the pseudogap region, from angular magnetoresistivity (AMR) measurements on $Y_{1-x}Pr_xBa_2Cu_3O_{7-\delta}$ single crystals, a system which exhibits typical pseudogap behavior [9] below a certain x -dependent temperature T^* . Even though magnetoresistivity is a second order effect with a very weak signal above T_{c0} and with the dissipative part due to vortex motion even weaker, angular magnetoresistivity makes it possible to discriminate between signals coming from the movement of vortices and of quasiparticles. Specifically, the angular dependent in-plane magnetoresistivity of the $x \geq 0.2$ single crystals displays a deviation

from the typical $\sin^2\theta$ dependence over a certain temperature range in the pseudogap region. We show that this deviation is a result of the presence of a flux-flow type contribution to magnetoresistivity in this T range. These results are consistent with the existence of vortexlike excitations in the pseudogap region, up to a temperature T_ϕ , that manifest themselves as flux-flow resistivity, supporting the scenario in which the zero-field superconducting transition is the onset of only long-range phase coherence.

Single crystals of $Y_{1-x}Pr_xBa_2Cu_3O_{7-\delta}$ ($x = 0, 0.13, 0.2, 0.32, 0.42,$ and 0.46) with $35 \text{ K} \leq T_{c0} \leq 92 \text{ K}$, grown as described in Ref. [10] were investigated. The crystals have typical sizes of $1 \times 0.6 \times 0.03 \text{ mm}^3$, with the c axis oriented along the smallest dimension. In-plane ρ_{ab} and out-of-plane ρ_c resistivities were measured simultaneously using the multiterminal configuration. Specifically, a current $I \leq 0.1 \text{ mA}$ was applied on one face of the single crystal and the voltages on both faces were measured with a low frequency (16 Hz) ac bridge. The components of the resistivity tensor were extracted from these voltages using the algorithm described in Ref. [11]. The AMR $\Delta\rho_{ab}^{\text{anis}}/\rho_{ab} \equiv [\rho_{ab}(\theta) - \rho_{ab}(0)]/\rho_{ab}(0)$ was determined at constant temperature and applied magnetic field H up to 14 T (with θ the angle between H and the c axis) by rotating the single crystal from $H||c$ to $H||(ab)||I$.

Figure 1 shows the T dependence of the in-plane resistivity of the six $Y_{1-x}Pr_xBa_2Cu_3O_{7-\delta}$ single crystals studied. As expected, upon increasing Pr doping, the zero-field critical temperature T_{c0} (defined here as the temperature corresponding to the inflection point in the transition region) decreases from 92 K for the $x = 0$ sample to 35 K for the most underdoped sample. The reduction of T_{c0} is accompanied by an increase in the magnitude of ρ_{ab} , indicating decreasing charge carrier concentration with increasing Pr doping. The in-plane resistivity of the $x = 0$ single crystal changes with T slightly faster than linear; i.e., ρ_{ab} is best fitted to a

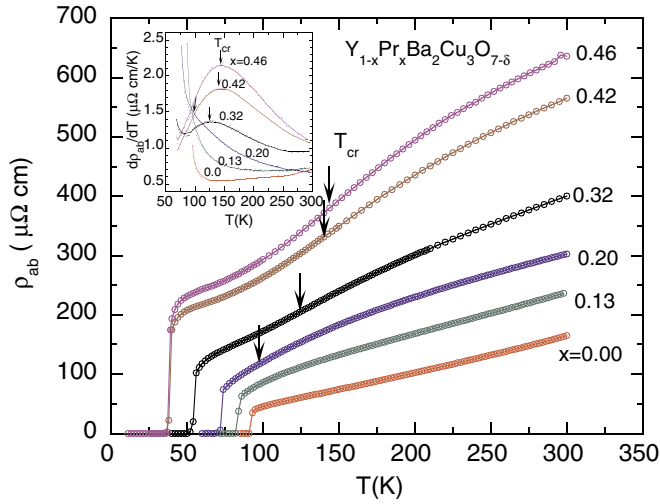


FIG. 1 (color online). Temperature T dependence of in-plane resistivity ρ_{ab} of $Y_{1-x}Pr_xBa_2Cu_3O_{7-\delta}$ single crystals with different Pr doping, measured in zero magnetic field. Inset: temperature T dependence of the temperature derivative of in-plane resistivity $d\rho_{ab}/dT$. The solid lines are guides to the eye. The arrows in both the main panel and the inset mark the positions of the inflection points T_{cr} in $\rho_{ab}(T)$ dependence.

combination of T and T^2 , suggesting slight overdoping. A linear increase in $\rho_{ab}(T)$ with increasing T is present for the $x = 0.13$ sample at temperatures $T \geq 175$ K. The T range of the linear $\rho_{ab}(T)$ regime shifts towards higher temperatures with increasing Pr doping, i.e., $T \geq 260$ K for the $x = 0.2$ sample and $T > 300$ K at higher Pr doping. Hence, for the $x = 0.32, 0.42,$ and 0.46 samples, $\rho_{ab}(T)$ is nonlinear for $T \leq 300$ K, displaying the pseudogap regime for all measured temperatures above T_{c0} .

The AMR was measured at different magnetic fields and temperatures. The angular magnetoresistivity of the $x = 0.32$ single crystal ($T_{c0} = 55$ K) measured at 60 and 105 K in a magnetic field of 14 T is shown in Fig. 2(a) and its left inset, respectively. The in-plane resistivity is larger when $H \parallel c$ axis ($\theta = 0^\circ$) than when H is applied along the current in the ab plane ($\theta = 90^\circ$). Also, $\Delta\rho_{ab}^{anis}/\rho_{ab}$ exhibits the expected $\sin^2\theta$ dependence, a result of quasiparticle dissipation, for $T \geq 105$ K. Indeed, notice the excellent fit of the 105 K data of the left inset with a $\sin^2\theta$ dependence (solid curve). However, a deviation from this angular dependence appears at lower temperatures as exemplified by Fig. 2(a), in which a $\sin^2\theta$ dependence (solid curve) gives a very poor fit of the data. This deviation from $\sin^2\theta$ dependence becomes more conspicuous around and below T_{c0} (notice the fast decrease of the data of Fig. 2(b) around 90° with decreasing T). The angular dependence depicted by this concentration is common to all samples with $x \geq 0.20$. The fast decrease of the resistivity, hence AMR, in the vicinity of $\theta = 90^\circ$ could arise only if a dissipative process that contributes to resistivity is suppressed when the field becomes parallel to

the ab planes. Such a process is similar to the lock-in transition of the flux lines in a layered superconductor when the intrinsic pinning and/or the cancellation of the Lorentz force suppresses the flow of the vortices. This suggests that the deviation of AMR from $\sin^2\theta$ could be a result of flux-flow dissipation.

Starting from this observation, we write the total conductivity above T_{c0} as a sum of quasiparticle and flux-flow contributions, i.e., $\sigma(T, H, \theta) \equiv \sigma_{qp}(T, H, \theta) + \rho_{FF}^{-1}(T, H, \theta)$. Within Boltzmann's approximation, the quasiparticle conductivity is:

$$\sigma_{qp}(T, H, \theta) \equiv \sigma_0 - \sigma^{(2)}H^2\cos^2\theta, \quad (1)$$

where σ_0 and $\sigma^{(2)}$ are the first two terms of the Jones-Zener series of the conductivity in powers of H . The angular dependence of the flux-flow resistivity is given

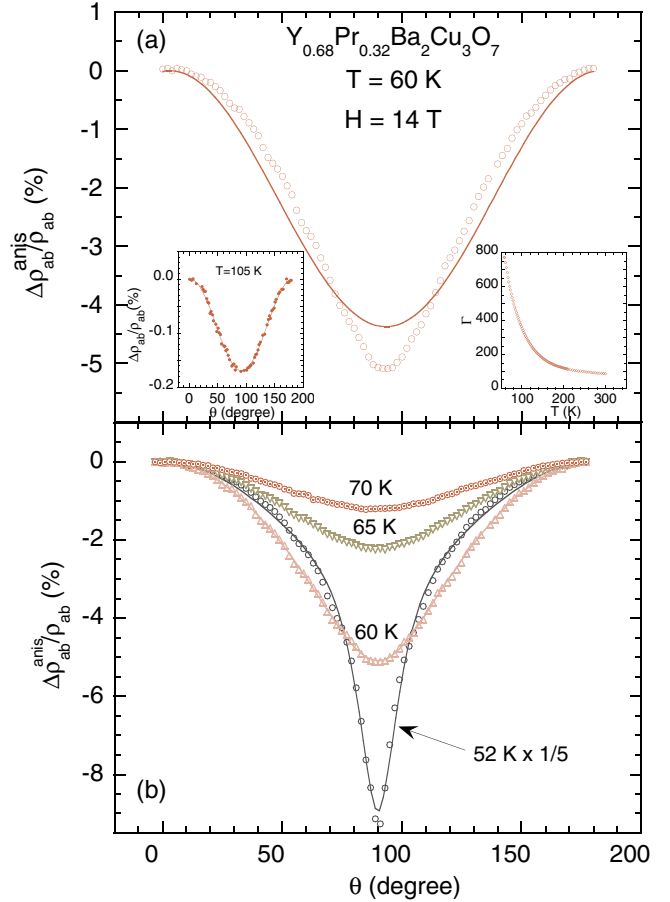


FIG. 2 (color online). Plot of angular in-plane magnetoresistivity $\Delta\rho_{ab}^{anis}/\rho_{ab} \equiv [\rho_{ab}(\theta) - \rho_{ab}(0)]/\rho_{ab}$ vs angle θ between the magnetic field H and the c axis, measured at 14 T and 60 K (a) and 105 K (left inset) for the $x = 0.32$ single crystal ($T_{c0} = 55$ K). Right inset: temperature dependence of resistive anisotropy Γ . The solid lines are $\sin^2\theta$ fits of the data. (b) Angular dependence of $\Delta\rho_{ab}^{anis}/\rho_{ab}$ measured around the superconducting transition temperature. The solid lines are fits of the data with Eq. (3).

by [12]

$$\rho_{\text{FF}} \equiv \rho_0 H \sum_i \frac{p_i}{\eta_i H_{c2}^i(T, \theta = 0)} |\cos \theta| \sqrt{\cos^2 \theta + \Gamma^{-1} \sin^2 \theta} + \beta \rho_{\text{qp}}, \quad (2)$$

where p_i is the weight of the superconducting regions

$$\frac{\Delta \rho_{ab}^{\text{anis}}}{\rho_{ab}} \approx -\frac{\Delta \sigma_{ab, \text{qp}}}{\sigma_{ab}} - \frac{\Delta \sigma_{ab, \text{FF}}}{\sigma_{ab}} = -M_{\text{qp}}(T, H) \sin^2 \theta - \frac{1}{M_{\text{FF}} |\cos \theta| \sqrt{\cos^2 \theta + \Gamma^{-1} \sin^2 \theta} + \beta(1 + M_{\text{qp}} \cos^2 \theta)} + \frac{1}{M_{\text{FF}} + \beta(1 + M_{\text{qp}})}. \quad (3)$$

Here $M_{\text{qp}}(T, H) \equiv \sigma_{\text{qp}}^{(2)} H^2 / \sigma_0$ and $M_{\text{FF}}(T, H) \equiv H \sum_i [p_i / \eta_i H_{c2}^i(T, \theta = 0)]$ are temperature and field dependent coefficients for the quasiparticle and flux-flow terms, respectively, and $\Gamma(T) \equiv \rho_c / \rho_{ab} \gg 1$ is the temperature dependent resistive anisotropy [see right inset in Fig. 2(a)]. We note that the value of $\Gamma^{1/2} \approx 28$ close to the superconducting transition temperature is consistent with the lower limit for the superconducting anisotropy $\gamma \equiv \lambda_c / \lambda_{ab} \approx 18$ for an equivalent doping state, as obtained from the temperature dependence of the melting field [14].

Equation (3) gives an excellent fit to the measured in-plane angular magnetoresistivity for all $x \geq 0.20$ single crystals [see solid lines in Fig. 2(b) for the $x = 0.32$ sample] for $T \leq T_\phi$. However, the in-plane angular magnetoresistivity displays *only* a $\sin^2 \theta$ dependence for the $x = 0$ and 0.13 samples over the whole measured T range, and for the $x \geq 0.2$ single crystals for $T > T_\phi$.

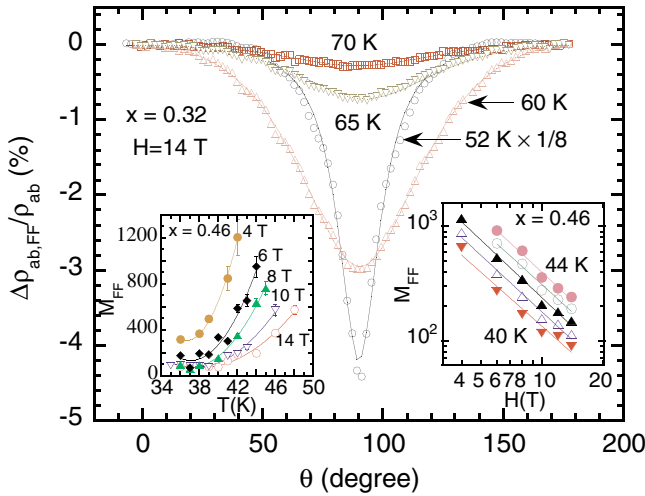


FIG. 3 (color online). Angular dependence of flux-flow magnetoresistivity $\Delta \rho_{ab, \text{FF}} / \rho_{ab}$ for the $x = 0.32$ single crystal ($T_{c0} = 55$ K) measured around the superconducting transition temperature. The solid lines are fits of the data with the flux-flow terms of Eq. (3). Plot of the flux-flow coefficient M_{FF} of Eq. (3) vs temperature T (left inset) and magnetic field (right inset) for the $x = 0.46$ single crystal ($T_{c0} \approx 35$ K and $T_\phi \approx 1.5 \times T_{c0}$). The lines are guides to the eye.

with an upper critical field H_{c2}^i . Here, we added the second term $\beta \rho_{\text{qp}}$ to the flux-flow resistivity in order to account for the serial resistances connecting nonpercolating superconducting regions along a current path. The coefficients p_i , η_i , and β are temperature and field dependent. The angular magnetoresistivity is then given by [13]

Figure 3 shows the extracted flux-flow magnetoresistivity, obtained by subtracting the quasiparticle magnetoresistivity from the measured magnetoresistivity, for the $x = 0.32$ single crystal ($T_{c0} \approx 55$ K and $T_\phi \approx 1.9 \times T_{c0}$) for temperatures above and below T_{c0} . Notice that the data display the typical dip for the flux-flow contribution at 90° [$H \parallel (ab)$], where the dissipation is strongly suppressed. Also, the magnitude of the flux-flow magnetoresistivity increases sharply (the magnitude of the dip increases) below T_{c0} , where flux-flow is the dominant dissipative process. The solid lines are fits of the data with the flux-flow terms of Eq. (3). Such an angular dependence is typical for scaling fields of anisotropic superconductors, in this case the upper critical field. Also, $\Delta \rho_{ab, \text{FF}} / \rho_{ab}$ has the same angular dependence both below and above T_{c0} . All these results clearly indicate the presence of vortexlike excitations well above T_{c0} , supporting the scenario in which the zero-field superconducting transition is just the result of long-range phase coherence. We also note that the dip becomes less sharp with increasing T . This rounding of the dip with increasing T is the effect of thermal fluctuations that produce a transverse diffusion of the field-induced vortex lines. The smearing is more prominent at low fields (4–8 T) [15].

The plots of the fitting parameter M_{FF} as a function of T and H are shown in the left and right insets, respectively, in Fig. 3. The flux-flow like term M_{FF} increases (decreases) with increasing temperature (magnetic field). $M_{\text{FF}}(H)$ follows a power-law dependence with a power of -1.5 at temperatures between 40 and 45 K. The observed $M_{\text{FF}}(T, H)$ could be explained as follows. On one hand, with increasing temperature or magnetic field, the vortex cores expand [$dH_{c2}(T)/dT$ is negative] or the number of vortices increases, respectively. Consequently, the flux-flow dissipation increases. On the other hand, at $T > T_{c0}$ and high magnetic fields, the number of regions able to support vorticity is not constant but decreases with increasing T and H . Therefore, the dissipation decreases. The overall effect is an increase (decrease) of M_{FF} with increasing temperature (magnetic field). The minimum observed in $M_{\text{FF}}(T)$ close to T_{c0} could have its origin in

the crossover of $\eta(T)$ in this region from $\eta \propto (1 - T/T_c)^{-1/2}$ to $\eta \propto (1 - T/T_c)^{1/2}$. This crossover occurs when the diffusion and inelastic relaxation rates become comparable [12].

The presence of vortices above the critical temperature requires a sufficient density of Cooper pairs to support vortexlike correlations. In this scenario, above T_{c0} , there are strong phase fluctuations of the superconducting order parameter boosted by the low stiffness energy $\hbar^2 n_s d / (4m_0^*)$ (with d the interlayer distance and m_0^* the effective mass of charge carriers). Moreover, due to the layered structure of the cuprates, the phase correlator decays algebraically [16] rather than exponentially as in three-dimensional (3D) superconductors. However, above a certain temperature T_ϕ , the Gorkov pairing amplitude decreases below the sustainability of vortex excitations. Meingast *et al.* [17] estimated this temperature to be roughly $1.5 \times T_{c0}$ and $2 \times T_{c0}$ for 3D and nearly 2D systems, respectively, based on an anisotropic 3D-XY model. The present study shows that, indeed, $1.5 \times T_{c0} \leq T_\phi \leq 2 \times T_{c0}$, depending on the anisotropy of the sample. Hence, for $T > T_\phi$, vortices can no longer exist, although Cooper pairs could persist up to temperatures as high as the pseudogap temperature $T^* > T_\phi$, as had been found in high field transport measurements [18,19]. Therefore, in this picture, T_ϕ is the temperature below which the number of Cooper pairs reaches a critical value, which makes them able to support vortex correlations but not long-range phase correlations.

Finally, we discuss the temperature dependence of the zero-field in-plane resistivity in the context of the presence of thermally generated vortices above the superconducting critical temperature. The temperature derivative $d\rho_{ab}/dT$ of the resistivity is positive and has a maximum that shifts to higher temperatures with increasing Pr content (inset to Fig. 1). ρ_{ab} depends on the density of states (DOS) at the nodal points in the momentum space, which practically are not affected by the opening of the pseudogap. Therefore, $d\rho_{ab}/dT$ should be positive and increase with decreasing T , as indeed it does, down to the peak temperature T_{cr} . Its decrease for $T < T_{cr}$ indicates that a new dissipative mechanism appears below T_{cr} . The most likely source of dissipation comes from the thermally excited vortex loops.

In conclusion, angular magnetoresistivity measured in magnetic fields up to 14 T on $Y_{1-x}Pr_xBa_2Cu_3O_{7-\delta}$ single crystals with $x \geq 0.2$ displays a deviation from $\sin^2\theta$ dependence (typical for quasiparticles) below a certain temperature T_ϕ , in the pseudogap region. We show that this deviation is a result of the presence of a flux-flow type contribution to magnetoresistivity. Therefore, these results are consistent with the existence of vortexlike excitations above the zero-field critical temperature T_{c0} , supporting the assumption that T_{c0} in underdoped cup-

rates is rather a phase ordering temperature than a mean field transition temperature. The presence of vortices above T_{c0} in underdoped cuprates raises questions regarding their core structure and quasiparticle spectrum, as well as their distribution within the material, which needs to be investigated.

This research was supported by the National Science Foundation under Grant No. DMR-0406471 at KSU and the US Department of Energy under Grant No. DE-FG03-86ER-45230 at UCSD.

*Permanent address: National Institute of Materials Physics, R76900 Bucharest, Romania.

†Present address: Department of Physics and Astronomy, State University of NY at Stony Brook, Stony Brook, NY 11994, USA.

- [1] A. A. Abrikosov, Zh. Eksp. Teor. Fiz. **32**, 1442 (1957) [Sov. Phys. JETP **5**, 1774 (1957)].
- [2] V. J. Emery and S. A. Kivelson, Nature (London) **374**, 434 (1995); Phys. Rev. Lett. **74**, 3253 (1995).
- [3] M. Franz and A. J. Millis, Phys. Rev. B **58**, 14572 (1998).
- [4] H.-J. Kwon and A. T. Dorsey, Phys. Rev. B **59**, 6438 (1999).
- [5] M. Franz and Z. Tesanovic, Phys. Rev. Lett. **87**, 257003 (2001).
- [6] J. Corson, R. Malozzi, J. Orenstein, J. N. Eckstein, and L. Bozovic, Nature (London) **398**, 221 (1999).
- [7] Z. A. Xu, N. P. Ong, Y. Wang, T. Kageshita, and S. Uchida, Nature (London) **406**, 486 (2000); Y. Wang, Z. A. Xu, T. Kageshita, S. Uchida, S. Ono, Y. Ando, and N. P. Ong, Phys. Rev. B **64**, 224519 (2001).
- [8] A. Lascialfari, A. Rigamonti, L. Romano, P. Tedesco, A. Varlamov, and D. Embriaco, Phys. Rev. B **65**, 144523 (2002).
- [9] M. B. Maple, J. Magn. Magn. Mater. **177**, 18 (1998).
- [10] L. M. Paulius, B. W. Lee, M. B. Maple, and P. K. Tsai, Physica C (Amsterdam) **230**, 255 (1994).
- [11] C. N. Jiang, A. R. Boldwin, G. A. Levin, T. Stein, C. C. Almasan, D. A. Gajewski, S. Han, and M. B. Maple, Phys. Rev. B **55**, R3390 (1997).
- [12] N. Kopnin, *Theory of Nonequilibrium Superconductivity* (Clarendon Press, Oxford, 2001), p. 238–252.
- [13] E. Cimpoiasu, G. A. Levin, C. C. Almasan, H. Zheng, and B. W. Veal, Phys. Rev. B **63**, 104515 (2001).
- [14] C. C. Almasan and M. B. Maple, Phys. Rev. B **53**, 2882 (1996).
- [15] T. Chen and S. Teitel, Phys. Rev. B **55**, 15197 (1997).
- [16] B. A. Bernevig, Z. Nazario, and D. I. Santiago, cond-mat/0304419.
- [17] C. Meingast, V. Pasler, P. Nagel, A. Rykov, S. Tajima, and P. Olsson, Phys. Rev. Lett. **89**, 229704, (2002).
- [18] T. Shibauchi, L. Krusin-Elbaum, M. Li, M. P. Maley, and P. H. Kes, Phys. Rev. Lett. **86**, 5763 (2001).
- [19] L. Krusin-Elbaum, T. Shibauchi, and C. H. Mielke, Phys. Rev. Lett. **92**, 097005 (2004).